HHS Public Access

Author manuscript

Cell Rep. Author manuscript; available in PMC 2016 March 14.

Published in final edited form as:

Cell Rep. 2016 March 1; 14(8): 1953–1965. doi:10.1016/j.celrep.2016.01.064.

Ezh2 Controls an Early Hematopoietic Program and Growth and Survival Signaling in Early T Cell Precursor Acute Lymphoblastic Leukemia

Etienne Danis[1,6], **Taylor Yamauchi**[1,6], **Kristen Echanique**[1], **Xi Zhang**[1], **Jessica N. Haladyna**[1], **Simone S. Riedel**[1], **Nan Zhu**[2], **Huafeng Xie**[3], **Stuart H. Orkin**[3], **Scott A. Armstrong**[4], **Kathrin M. Bernt**[1,5,7,*], and **Tobias Neff**[1,5,7,*]

[1]Department of Pediatrics, Section of Pediatric Hematology/Oncology/Bone Marrow Transplantation, University of Colorado Denver, Aurora, CO 80045, USA

[2]Stem Cell Biology and Hematopoiesis Program, Blood Research Institute, Blood Center of Wisconsin, Milwaukee, WI 53226, USA

[3]Dana Farber Cancer Institute and Boston Children's Hospital, Harvard Medical School and HHMI, Boston, MA 02115, USA

[4]Cancer Biology and Genetics Program, Departments of Medicine and Pediatrics, Memorial Sloan Kettering Cancer Center, New York, NY 10065, USA

[5]Center for Cancer and Blood Disorders, Children's Hospital Colorado, Aurora, CO 80045, USA

SUMMARY

Early T cell precursor acute lymphoblastic leukemia (ETP-ALL) is an aggressive subtype of ALL distinguished by stem-cell-associated and myeloid transcriptional programs. Inactivating alterations of Polycomb repressive complex 2 components are frequent in human ETP-ALL, but their functional role is largely undefined. We have studied the involvement of *Ezh2* in a murine model of *NRASQ61K*-driven leukemia that recapitulates phenotypic and transcriptional features of ETP-ALL. Homozygous inactivation of *Ezh2* cooperated with oncogenic NRASQ61K to accelerate leukemia onset. Inactivation of *Ezh2* accentuated expression of genes highly expressed

*Correspondence: kathrin.bernt@ucdenver.edu (K.M.B.), tobias.neff@ucdenver.edu (T.N.).
[6]Co-first author
[7]Co-senior author

AUTHOR CONTRIBUTIONS

E.D., T.Y., S.H.O., S.A.A, K.M.B, and T.N. designed the study. E.D., T.Y., X.Z., K.E., J.N.H., N.Z., S.S.R., H.X., K.M.B., and T.N. performed experiments. H.X., S.H.O., S.A.A., and T.N. generated reagents used in experiments. E.D., T.Y., K.M.B., and T.N. analyzed the data. E.D.,T.Y., T.N., and K.M.B. prepared the manuscript with input from the other authors.

ACCESSION NUMBERS

The accession number for the RNA-seq and ChIP-seq data reported in this paper is GEO: GSE76603.

SUPPLEMENTAL INFORMATION

Supplemental Information includes Supplemental Experimental Procedures, seven figures, and one table and can be found with this article online at http://dx.doi.org/10.1016/j.celrep.2016.01.064.

in human ETP-ALL and in normal murine early thymic progenitors. Moreover, we found that *Ezh2* contributes to the silencing of stem-cell- and early-progenitor-cell-associated genes. Loss of *Ezh2* also resulted in increased activation of STAT3 by tyrosine 705 phosphorylation. Our data mechanistically link *Ezh2* inactivation to stem-cell-associated transcriptional programs and increased growth/survival signaling, features that convey an adverse prognosis in patients.

Graphical Abstract

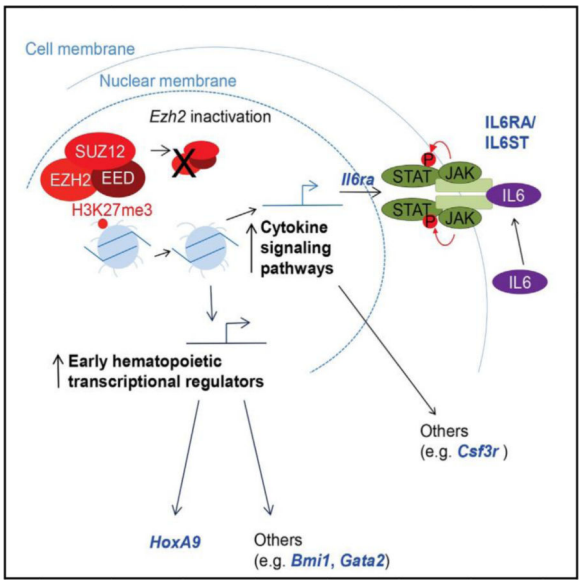

INTRODUCTION

Both gain and loss of function of developmental regulator Polycomb repressive complex 2 (PRC2) are found in cancer, including leukemia and lymphoma. The underlying mechanisms are incompletely understood. PRC2 consists of the core subunits Extraembryonic Ectoderm Development (*EED*), Suppressor of Zeste 12 (*SUZ12*), and the methyltransferase Enhancer of Zeste 2 (*EZH2*) (reviewed in Laugesen and Helin, 2014). High-level expression of *EZH2* has been described in prostate cancer and other epithelial malignancies (Varambally et al., 2002), and hyperactive mutants of *EZH2* have been identified in diffuse large B cell lymphoma (DLBCL) and follicular lymphoma (FL) (Okosun et al., 2014; Sneeringer et al., 2010). On the other hand, *EZH2* is somatically inactivated in other hematological malignancies, including myelodysplastic syndrome (MDS), myeloproliferative neoplasm (MPN), and CALM-AF10 leukemia (Ernst et al., 2010; Grossmann et al., 2012; Guglielmelli et al., 2011; Nikoloski et al., 2010). PRC2 components are also inactivated by mutation in T-lineage acute lymphoblastic leukemia (ALL) (Ntziachristos et al., 2012), and especially in the aggressive subtype early T cell precursor (ETP)-ALL (Zhang et al., 2012a). Alterations of the methyltransferase EZH2 in particular have been linked to poor clinical outcomes in this disease (Zhang et al., 2012a).

Data from animal models have provided some insight into the role of PRC2 in normal development and malignancy without resolving how both gain and loss of function of PRC2

contribute to the development of hematologic malignancies. The PRC2 core components *Ezh2*, *Suz12*, and *Eed* are required for proper differentiation of mouse embryonic stem cells (Pasini et al., 2007; Shen et al., 2008). The causal involvement of hyperactive *Ezh2* mutations in lymphomagenesis has been demonstrated in mice (Béguelin et al., 2013; Caganova et al., 2013). At the same time, *Ezh2* is required for proper B and T cell development (Su et al., 2005). Inactivation of *Ezh2* is partially compensated in some contexts by the less well-characterized methyltransferase EZH1 (Margueron et al., 2008; Shen et al., 2008), whereas inactivation of *Eed* leads to complete loss of the canonical PRC2 function and di- and tri-methylation of lysine 27 on histone 3 (Shen et al., 2008; Xie et al., 2014). Inactivation of *Ezh2* and *Eed* both impair the growth of murine models of *MLL*-rearranged acute myeloid leukemia (AML), and this effect has been ascribed in part to derepression of the *Cdkn2a* tumor suppressor encoding $p16^{ink4a}$ and $p19^{arf}$ (Neff et al., 2012; Shi et al., 2013). In contrast, inactivation of *Ezh2* in mice has led to T cell leukemia (Simon et al., 2012) and MDS/MPN-like conditions (Muto et al., 2013). To better understand how PRC2 functions as a tumor suppressor in ETP-ALL, we developed a murine model that recapitulates features of human ETP-ALL and directly compared leukemias with and without inactivation of *Ezh2 and Eed*.

RESULTS

NRASQ61K-Expression in *Cdkn2a*$^{-/-}$ Stem/Progenitor Cells Cooperates with Homozygous *Ezh2* or *Eed* Inactivation in Leukemogenesis

Human ETP-ALL is an aggressive subtype of ALL and has been linked to a stem-cell-like gene-expression program (Zhang et al., 2012a). Genetic changes occurring in ETP-ALL are heterogeneous, with inactivating mutations of PRC2-components occurring frequently and being linked to poor clinical outcomes (Zhang et al., 2012a). We sought to study the role of *Ezh2* in a mouse model mediated by genetic alterations found in human ETP-ALL. Many cases of ETP-ALL have alterations that directly (e.g., oncogenic mutations) or indirectly (e.g., NF1-inactivation) activate RAS signaling. *Cdkn2a* mutations/deletions are encountered in a subset of ETP-ALL. Among 64 ETP cases in the St. Jude study, there are 11 NRAS mutated ETP cases. 5 of the 11 NRAS mutant ETP cases have alterations in at least one PRC2 component (Zhang et al., 2012a).

To model human ETP-ALL, we introduced oncogenic *NRASQ61K* and a self-excising hit-and-run Cre or an inert GFP-expressing control vector (MSCV-ires-GFP = MIG) into *Ezh2*$^{f/f}$ *Cdkn2a*$^{-/-}$ *ROSA26lox-Stop-loxYFP* lineage-negative, SCA1-positive, and KIT-positive (LSK) cells (Neff et al., 2012; Serrano et al., 1996; Srinivas et al., 2001). Cells were expanded in the presence of cytokines promoting lymphoid development (SCF, FLT3L, and IL7) on OP9-DL1, a feeder cell line providing a Notch signal by expressing Delta-like 1 ligand. We chose a time window of 14 days to allow for expansion of cells and to approximate the time window (Schmitt and Zúñiga-Pflücker, 2002) reported to allow for T-lineage differentiation from immature hematopoietic cells using OP9-DL1 cells (Figure 1A). Cells grown in this manner for 14 days demonstrated a phenotype consistent with murine double-negative (DN) 1 and 2 cells in the setting of *Ezh2* inactivation, whereas the floxed counterparts showed a majority of cells progressing to the DN3 stage (Figures S1A–S1C).

Cells also had a surface marker profile consistent with human ETP leukemia, with subsets staining positive for MAC1 and/or GR1 (Figure S1D), CD5 (Figure S1E), and KIT (Figure S1F). *Ezh2*$^{f/f}$ *and Ezh2*$^{D/D}$ *Cdkn2a*$^{-/-}$ *NRASQ61K* cells were transplanted into recipient mice to interrogate their leukemogenic potential.

Cre-transduced *NRASQ61K Ezh2*$^{f/f}$ *Cdkn2a*$^{-/-}$ *ROSA26lox-Stop-loxYFP* cells were found to have fully excised floxed *Ezh2*-sequences at the time of injection (Figure S2A). In contrast, co-transduction of *NRASQ61K* and Cre into LSK cells with an intact *Cdkn2a* locus (*Ezh2*$^{f/f}$ *Cdkn2a*$^{+/+}$ LSK cells) resulted in outgrowth of incompletely *Ezh2*-excised cells (Figure S2B), and these cells were not transplanted in vivo. We documented loss of EZH2 in *Ezh2*$^{D/D}$ *Cdkn2a*$^{-/-}$ *NRASQ61K* cells at the protein level (Figure S2C). Excision of floxed *Ezh2* sequences led to globally reduced H3K27me2 (Figure S2D) and H3K27me3 (Figure 1B) in *Ezh2*$^{D/D}$ *Cdkn2a*$^{-/-}$ *NRASQ61K* cells compared to *Ezh2*$^{f/f}$ *Cdkn2a*$^{-/-}$ *NRASQ61K* cells.

Transplantation of *NRASQ61K*-transduced cells resulted in leukemia with 100% penetrance in the presence or absence of functional *Ezh2*; however, inactivation of *Ezh2* resulted in significantly shortened latency (Figure 1C). Sustained complete excision of floxed *Ezh2* sequences was documented in vivo by RNA-seq (Figure S2E) and by qRT-PCR (Figures S2F and S2G). Inactivation of the PRC2 component *Eed* (*Eed*$^{D/D}$ *Cdkn2a*$^{-/-}$ *NRASQ61K*) also resulted in significantly shortened eukemia latency (Figure 1D). Latency of *Eed*-inactivated and *Ezh2*-inactivated *NRASQ61K* leukemias on a *Cdkn2a*$^{-/-}$ background was very similar in a direct comparison (Figure 1E). Excision of floxed *Eed* sequences was confirmed by qRT-PCR (Figure S2H). Inactivation of *Eed* resulted in an expected global cellular loss of H3K27me3 (Figure S2I).

NRASQ61K Leukemia Shares Phenotypic Features with Human ETP-ALL

In addition to a shortened latency for leukemias with compromised PRC2 function, we observed subtle phenotypical differences that are consistent with more aggressive and immature disease. Recipients of *Ezh2*$^{D/D}$ *Cdkn2a*$^{-/-}$ *NRASQ61K* cells had significantly higher peripheral white blood cell counts and a trend toward lower hemoglobin and platelet counts (Figure S2J). Engraftment in the bone marrow (Figure S3A) of moribund mice was also higher in the *Ezh2*$^{D/D}$ and *Eed*$^{D/D}$ groups compared to floxed counterparts. There was no clear trend for splenic involvement: spleen weight (Figure S3B) was similar in the *Ezh2*$^{D/D}$ and slightly but significantly lower in the *Eed*$^{D/D}$ group; however, engraftment was higher in the *Ezh2*$^{D/D}$ and *Eed*$^{D/D}$ groups compared to floxed counterparts (Figure S3C). We found a non-significant trend toward lower thymus weights (Figure S3D) and significantly lower thymic engraftment (Figure S3E) in the *Ezh2*$^{D/D}$ and *Eed*$^{D/D}$ groups, which is in keeping with a low frequency of mediastinal tumors in human ETP-ALL (Coustan-Smith et al., 2009).

Floxed, *Ezh2*$^{D/D}$, and *Eed*$^{D/D}$ splenic blasts had a similar immunophenotype, with minor differences. All three groups had a similar proportion of blasts with at least one myeloid marker (MAC1 or GR1; Figure S3F). *Ezh2*$^{D/D}$ *Cdkn2a*$^{-/-}$ blasts had a higher proportion of blasts double positive (DP) for both MAC1 and GR1 (Figure 2A). Common to all three groups was a majority of leukemia cells with a CD44-positive/CD25-negative surface

phenotype (Figure 2B; similar to thymic DN1 cells). We also observed subset positivity for the lymphoid marker CD5 (Figure 2C) and for c-KIT (Figure 2D). The phenotype of *Ezh2*$^{f/f}$ *Cdkn2a*$^{-/-}$ and *Ezh2*$^{D/D}$ *Cdkn2a*$^{-/-}$ *NRASQ61K* leukemias was also similar with respect to expression of additional lymphoid surface markers (Figures S3G and S3H). However, *Ezh2*$^{f/f}$ *Cdkn2a*$^{-/-}$ cells had a higher proportion of CD8 single-positive cells (Figures S3I–S3L), consistent with a less stringent differentiation block. In summary, NRASQ61K-transformed murine LSK cells with an inactivated *Cdkn2a* locus form an acute leukemia in mice that shares phenotypic features with human ETP-ALL.

Ezh2-Inactivation Accentuates Transcriptional Programs Characteristic of ETP-ALL and of Normal Murine Early Thymic Precursors

To characterize the effects of *Ezh*2-inactivation on a molecular level, we performed global expression profiling by RNA-seq of *Ezh2*$^{D/D}$ and *Ezh2*$^{f/f}$ *Cdkn2a*$^{-/-}$ NRASQ61K cells both in vitro prior to transplantation and in vivo after harvest from leukemic spleens. Genes with increased expression in human ETP-ALL compared to typical T-lineage ALL (Zhang et al., 2012a) were significantly enriched in *Ezh2*$^{D/D}$ cells compared to *Ezh2*$^{f/f}$ counterparts (Figure 2E in vivo; Figure S3M in vitro). We also evaluated the expression of genes characteristic of purified, untransformed murine CD4/CD8 DN1 ETP cells compared to CD4/CD8 DP cells (Zhang et al., 2012b). This gene set was found to be enriched in *Ezh2*$^{D/D}$ compared to *Ezh2*$^{f/f}$ *Cdkn2a*$^{-/-}$ *NRASQ61K* cells in vivo (Figure 2F) and prior to transplantation (Figure S3N). We next investigated the link between the gene expression profile observed in *Ezh2*$^{D/D}$ *Cdkn2a*$^{-/-}$ *NRASQ61K* cells and genes that acquire H3K27me3 in the developmental transition from DN1 to DP ("DP_only_H3K27me3") as described previously (Zhang et al., 2012b). These PRC2 target genes are enriched in DN1 cells compared to DP cells (Figure S3O), consistent with a role for H3K27me3 in the maintenance of gene-repression during thymocyte development. We found this set of PRC2 target genes to also be enriched following *Ezh2*-inactivation in *Cdkn2a*$^{-/-}$ *NRASQ61K* cells (Figure 2G in vivo; Figure S3P in vitro). Importantly, one genomic site that is transcriptionally silenced in the transition from DN1 to DP cell and acquires H3K27me3 in this transition is the distal *HoxA* cluster (Figure 2H). Thus, *Ezh2* inactivation results in enhanced expression of genes that are highly expressed in human ETP-ALL and in murine purified DN1 ETP cells. Furthermore, *Ezh2* inactivation promotes expression of genes that acquire H3K27me3 in normal T-lineage development.

Differentiation Block of *NRASQ61K* Cells Is Partially Relieved by Thymic Microenvironment in Cells with Intact PRC2, but Not Cells with *Ezh2* or *Eed* Inactivation

Flow cytometric analysis of thymic fluorochrome-positive blasts demonstrated a significant proportion of CD4/CD8 DP blasts in recipients of cells with intact PRC2 function, but not recipients of *Ezh2*$^{D/D}$ *Cdkn2a*$^{-/-}$ *NRASQ61K* or *Eed*$^{D/D}$ *Cdkn2a*$^{-/-}$ *NRASQ61K* blasts (Figure 3A). PRC2-compromised cells also showed a lower proportion of CD44^{-}/CD25^{-} blasts (Figure 3B) and a significantly higher proportion of CD44^{+}/CD25^{-} (DN1- like) blasts (Figure 3C). All groups had similar levels of CD4 single-positive blasts (Figure 3D) and CD8 single-positive blasts (Figure 3E) in the thymus. Levels of KIT were slightly, but significantly, higher in recipients of *Ezh2*$^{D/D}$ cells (Figure 3F). These data show that the thymic microenvironment partially alleviates the differentiation block of NRASQ61K cells

in the presence of an intact PRC2 complex. The data further support the concept that PRC2 is important for thymic T cell differentiation and that impaired PRC2 function results in a differentiation block.

Genes Preferentially Marked by H3K27me3 in *Ezh2$^{f/f}$ Cdkn2a$^{-/-}$ NRASQ61K* Are Transcriptionally Enriched in *Ezh2$^{D/D}$* Cells

We performed chromatin immunoprecipitation sequencing (ChIP-seq) for H3K27me3 on cultured leukemias from recipients of *Ezh2$^{f/f}$* and *Ezh2$^{D/D}$ Cdkn2a$^{-/-}$ NRASQ61K* cells. There was notable loss of K27me3 signal in Ezh2-inactivated cells at loci with strong positive signal in floxed counterparts (Figure 4A). Using MACS2 (Feng et al., 2012), we identified 59,289 peaks (corresponding to 7,334 genes) for the *Ezh2$^{f/f}$ Cdkn2a$^{-/-}$ NRASQ61K* cells compared to 660 peaks (corresponding to 259 genes) in the *Ezh2$^{D/D}$ Cdkn2a$^{-/-}$ NRASQ61K* cells (Table S1). The H3K27me3-associated genes within both groups showed highly significant overlap with MSigDb gene sets consisting of established PRC2 targets, and the most significant hit for both groups in the entire MSigDb database was “BENPORATH_ES_WITH_H3K27ME3” (data not shown). A gene set defined as genes with differentially higher H3K27me3 signal in floxed cells was significantly enriched in *Ezh2$^{D/D}$ Cdkn2a$^{-/-}$ NRASQ61K* cells in vivo (Figure 4B) and prior to injection (data not shown). We found significant overlap between genes losing H3K27me3 in *Ezh2*-inactivated cells and genes gaining H3K27me3 in the transition from DN1 to DP cells (Zhang et al., 2012b) (Figure 4C).

Inactivation of *Ezh2* Accentuates a Stem- and Progenitor-Associated Transcriptional Program

Since ETP-ALL has been linked to stem cell transcriptional programs, we asked if inactivation of *Ezh2* leads to enrichment of stem-cell-associated transcriptional programs. We found that genes upregulated in human HSC (data from Novershtern et al., 2011; Figure 5A) and genes upregulated in murine HSC (data from Chambers et al., 2007; Figure 5B) compared to more mature cell types are enriched in *Ezh2$^{D/D}$ Cdkn2a$^{-/-}$ NRASQ61K* cells in vivo. We found enrichment of the same gene sets in *Ezh2$^{D/D}$ Cdkn2a$^{-/-}$ NRASQ61K* cells prior to injection (data not shown) and interestingly also in publically available expression data in *Ezh2$^{D/D}$* compared to *Ezh2$^{f/f}$* murine granulocyte-macrophage progenitors (GMPs) (data not shown) (Muto et al., 2013). These data provide additional evidence that *Ezh2* contributes to silencing of a stem-cell- and early-progenitor-cell-associated program in leukemic and normal hematopoiesis. We further confirmed increased expression of two stem-cell- and early-progenitor-cell-associated genes, *HoxA9* (Figure 5C) and *Bmi1* (Figure 5D), in response to *Ezh2* inactivation in vivo. These loci are PRC2 targets in *Ezh2$^{f/f}$ Cdkn2a$^{-/-}$ NRASQ61K* cells (Figure 5E). In summary, these data show that developmental transcriptional downregulation of stem-cell- and early- progenitor-cell-associated genes is accompanied by gain of H3K27me3 at a number of critical loci. Genetic inactivation of *Ezh2* leads to impairment in the developmentally regulated downregulation of these stem-cell- and early-progenitor-cell-associated genes. Thus, acquisition of the *Ezh2*-catalyzed H3K27me3 is associated with transcriptional silencing of stem-cell-associated programs during hematopoietic differentiation.

Forced Expression of *HoxA9* Recapitulates Key Aspects of PRC2 Inactivation

We confirmed that *HoxA9* is indeed a direct PRC2 target in our system using ChIP followed by qPCR (Figure 6A). Furthermore, genes with expression levels that correlate with *HOXA9* expression in T-ALL (including ETP-ALL) and in acute myeloid leukemia were identified using Pearson correlation analysis on two independent publically available human leukemia datasets (GSE28703, Zhang et al., 2012a; and GSE689, Verhaak et al., 2009), as previously described (Velu et al., 2014). Both gene sets clustered murine LSKs, GMPs, and megakaryocyte-erythroid progenitors (MEPs) with 100% accuracy, based on published expression data (Krivtsov et al., 2006, 2013) (Figure S4A). Genes correlated with *HOXA9* in T-ALL or AML were significantly enriched in *Ezh2*$^{D/D}$ versus *Ezh2*$^{f/f}$ *Cdkn2a*$^{-/-}$ *NRASQ61K* cells in vivo (Figures 6B and 6C) and prior to injection (Figures S4B and S4C).

We next asked if the elevated expression of the late *HoxA*-cluster gene *HoxA9* has functional relevance in our leukemia model. We coexpressed *HoxA9*-IRES-GFP or empty-vector-IRES-GFP with *NRASQ61K* in *Ezh2*$^{f/f}$ *Cdkn2a*$^{-/-}$ LSK cells. Cells were expanded on OP9-DL1 stroma in the presence of cytokines, and transplanted into syngeneic, sublethally irradiated recipients. Leukemia latency was shortened significantly in the recipients of *HoxA9*-overexpressing cells (Figure 6D). Overexpression of *HoxA9* was confirmed by qRT-PCR prior to injection (Figure 6E). We also noted enrichment of *HOXA9*-correlated genes in human ETP-ALL with genomic alteration in a PRC2 component compared to ETP-ALL without genomic alteration in PRC2 components (Figures S4D and S4E; data from Zhang et al., 2012a).

Ezh2$^{D/D}$ *Cdkn2a*$^{-/-}$ *NRASQ61K* Leukemias Show Accentuated Growth and Survival Signaling

While increased expression of a stem cell program, that includes HOXA cluster genes, explains a substantial portion of the phenotypic and transcriptional consequences of PRC2 inactivation, we also noted transcriptional evidence of increased growth and survival signaling in our transcriptome analysis. Dysregulated growth and survival signaling have previously been reported as a consequence of PRC2 inactivation. We performed gene set enrichment analysis (GSEA) in our ETP-ALL model and noted significant enrichment of growth factor and cognate receptor gene transcripts in *Ezh2*$^{D/D}$ *Cdkn2a*$^{-/-}$ *NRASQ61K* leukemias compared to floxed counterparts in vivo (Figure S5A) and in vitro (data not shown). In NF1 sarcomas, PRC2 inactivation has recently been linked to hyperactive RAS signaling and may occur at the chromatin level rather than through defined enhanced phospho-signaling (De Raedt et al., 2014). Indeed, we found RAS signatures accentuated in our model upon *Ezh2* inactivation (Figure S5B and data not shown). In addition, genes downregulated in NF1-associated sarcoma cell lines by reintroduction of *SUZ12* are enriched in our model upon *Ezh2*-inactivation (Figure S5C). Many of the genes deregulated in our model are documented targets of the STAT3 signaling pathway (Figures S5D and S5E). Furthermore, STAT3 is a critical component in myeloid development (McLemore et al., 2001; Shimozaki et al., 1997), in keeping with a myeloid surface marker phenotype in the *NRASQ61K* model. We therefore performed phospho-western blotting and documented increased phosphorylation of STAT3 on tyrosine residue 705 (Figure 7A). This raised the

intriguing possibility that PRC2 mutant ETP-ALL might be susceptible to JAK/STAT pathway inhibition even in the absence of mutations directly involved in the pathway.

Ezh2$^{D/D}$ *Cdkn2a*$^{-/-}$ *NRASQ61K* Cells Respond to JAK/STAT Pathway Inhibition

Phosphorylation of STAT3 and STAT5 has been recently been documented in a majority of human ETP-ALL, and was reversed by the JAK1/2 inhibitor ruxolitinib (Maude et al., 2015). Activating mutations in cytokine receptors that signal through JAK/STAT are found at substantial frequencies in human ETP-ALL, providing a rationale for the use of ruxolitinib in these subtypes. While our model does not carry any mutations that would be expected to signal through JAK/STAT, the increased STAT3Y705 phosphorylation led us to assess whether this pathway is functionally important in our ETP-ALL model. We exposed *Ezh2*$^{f/f}$ and *Ezh2*$^{D/D}$ *Cdkn2a*$^{-/-}$ *NRASQ61K* cells in vitro to ruxolitinib and observed that ruxolitinib reverses STAT3Y705 phosphorylation in both cell types (Figure 7B). In addition, ruxolitinib inhibited in vitro growth of *Ezh2*$^{D/D}$ *Cdkn2a*$^{-/-}$ *NRASQ61K* (Figure 7C). However, the increased STAT3Y705 phosphorylation in *Ezh2*$^{D/D}$ *Cdkn2a*$^{-/-}$ *NRASQ61K* did not confer hypersensitivity to ruxolitinib. Rather, loss of PRC2 appeared to be a possible mechanism of resistance, with higher doses of ruxolitinib being required to fully block STAT3Y705 phosphorylation and affect cell growth. Similar results were found in a second set of leukemias (Figure S5F). *Eed*$^{D/D}$ *Cdkn2a*$^{-/-}$ *NRASQ61K* cells likewise had accentuated phospho-STAT3Y705 (Figure S5G) and showed cell growth inhibition in response to ruxolitinib (Figure S5H). To further investigate the role of JAK/STAT signaling in our model, we evaluated the effect of two published STAT3 inhibitors, LLL12 (Liu et al., 2010) and BP-1-102 (Zhang et al., 2012c). Both inhibited STAT3Y705 phosphorylation in *Ezh2*$^{D/D}$ *Cdkn2a*$^{-/-}$ *NRASQ61K* cells and interfered with their growth (Figures S5I and S5J). In summary, these data provide strong evidence for the functional importance of JAK/STAT signaling in our model and raise concerns that PRC2 loss may make clinically meaningful inhibition of JAK/STAT signaling more challenging.

De-repression of *Il6ra* Contributes to Hyperactive JAK/STAT Signaling in T-ALL with PRC2 Inactivation

Finally, to better understand the mechanistic basis of the increased JAK/STAT signaling in *Ezh2*$^{D/D}$ versus *Ezh2*$^{f/f}$ *Cdkn2a*$^{-/-}$ *NRASQ61K* cells, we first asked whether STAT3 is transcriptionally upregulated in response to *Ezh2* inactivation. *Ezh2*$^{D/D}$ cells displayed slightly higher levels of *Stat3* mRNA (Figure S6A), though the effect was small and not statistically significant. We therefore assessed the responsiveness of our paired leukemias to several growth factors (FLT3L, HGF, IL6, IL7, and SCF). We found no difference in the responsiveness to FLT3L, HGF, and SCF (Figure S6B). However, both IL6 and IL7 led to exaggerated STAT3Y705 phosphorylation, with a very pronounced increase for IL6 (Figures 7D and S6B). *Il6ra* was significantly higher expressed in *Ezh2*-inactivated cells compared to floxed counterparts (Figure 7E). This finding correlates with higher levels of H3K27me3 at the *Il6ra* locus in *Ezh2*$^{f/f}$ compared to *Ezh2*$^{D/D}$ *Cdkn2a*$^{-/-}$ *NRASQ61K* leukemia by ChIP-seq (Figure 7F). *Il6ra* is transcriptionally downregulated in the transition from normal DN1 cells to DP cells, and the *Il6ra* locus acquires H3K27me3 in DP cells (Figure 7F) (Zhang et al., 2012b). The IL6R is also significantly higher expressed in ETP-ALL compared to typical ALL in the St. Jude study (Zhang et al., 2012a) (Figure 7G).

Increased STAT3Y705 phosphorylation due to IL6 hyper-responsiveness thus contributes to increased JAK/STAT signaling in *Ezh2*$^{D/D}$ T-ALL and may be a mediator of drug resistance to JAK1/2 inhibition in this model. Interestingly, we also observed an increase in STAT3Y705 phosphorylation in *Ezh2*$^{f/f}$ pre-leukemic and leukemic cells in HoxA9-overexpressing cells (Figure S6C), pointing toward a potential additional link between early hematopoietic transcriptional programs and accentuated signaling in our model.

DISCUSSION

The effects of PRC2 hyper- and hypoactivity in human disease and model systems have been contradictory. Hyperactive alleles of *EZH2* observed in human lymphomas contribute to differentiation block and lymphomagenesis in mouse models. Inactivation of *Ezh2* impedes the progression of *MLL-AF9* driven leukemia in mice (Neff et al., 2012; Tanaka et al., 2012), and inactivation of *Eed* is not tolerated (Neff et al., 2012; Shi et al., 2013). On the other hand, alterations in PRC2 components thought to be inactivating are associated with hematologic malignancies in hu- mans and mice. Recently, PRC2-mediated control of genes with opposing function on cellular growth has been demonstrated in normal murine hematopoiesis (Xie et al., 2014). Here, we provide evidence for the functional importance of *Cdkn2a* as an *Ezh2* downstream target in acute leukemia. Furthermore, our findings indicate that *Ezh2* has a functional role in the developmental silencing of a gene expression program associated with the transition of early thymic precursors to DP thymocytes and a transcriptional program associated with stem cells and early progenitor cells in normal hematopoiesis. We validated functional importance for one such gene, *HoxA9*, using an overexpression approach. Finally, we show that the prognostic implication of *Ezh2* alterations is in part explained by deregulated growth and survival signaling through STAT3, a signaling alteration also associated with other poor prognosis subsets of acute leukemia.

Control of Cdkns by *Ezh2*

Cdkn2a is an established binding target of PRC2 and PRC1. Previous studies have demonstrated that the adverse effects on cellular growth resulting from inactivation of *Eed* and other Polycomb-group genes in hematopoiesis can be rescued in part by genetic inactivation of *Cdkn2a* (Hidalgo et al., 2012; Oguro et al., 2012; Xie et al., 2014). Here, we report that genetic inactivation of *Cdkn2a* allows for the establishment of *Ezh2* null acute leukemia. In human ETP-ALL, PRC2 components are frequently altered, but *CDKN2A* is deleted in a minority of cases (Haydu and Ferrando, 2013; Zhang et al., 2012a). These data suggest that in human ETP-ALL, *CDKN2A* may be controlled by mechanisms other than deletional inactivation. In accord with this speculation, *CDKN2A* is a documented target of epigenetic silencing in human leukemia. It will be important to study how this locus is controlled in human ETP-ALL with impaired PRC2-function. Candidate mechanisms include DNA methylation, H3K9 methylation, and PRC1-dependent silencing.

Ezh2 Contributes to Developmental Silencing of Genes Expressed in Early T Cell Precursors and in Stem Cells and Early Progenitor Cells

The developmental transition from early thymic precursor to DP thymocyte has been well characterized. ETPs have been documented to retain myeloid development potential that is progressively lost in the transition to DP cell (Bell and Bhandoola, 2008; Wada et al., 2008). The developmental transition is accompanied by the acquisition of H3K27me3 at many loci, including stem-cell-associated genes such as late *HoxA*-cluster genes and the receptor for IL6 (Zhang et al., 2012b). These findings are in keeping with a recently described role for PRC2 and Ikaros in regulating thymocyte development (Oravecz et al., 2015). In our *NRASQ61K* leukemia model, *Ezh2*-inactivation results in enriched expression of genes associated with DN1 cells, and therefore contributes to a differentiation block.

Ezh2 Contributes to Developmental Silencing of Genes Highly Expressed in Early Hematopoiesis

We found that genes expressed in early hematopoiesis, such as HoxA9, Bmi1 (Figure 5E), and Gata2 (data not shown), are PRC2 targets in our model. We also noted that these genes are silenced and acquire H3K27me3 in the developmental transition from immature LSK to GMP cells in published data (data not shown) (Bernt et al., 2011). There is significant overlap in the genes acquiring H3K27me3 in the transition from LSK to GMP and in the transition from DN1 to DP, further supporting a role for Ezh2/PRC2 in the silencing of early transcriptional programs in hematopoietic differentiation (Figure S7). Epigenetic mechanisms have been implicated in the differentiation-associated silencing of genes highly expressed in the stem/early progenitor compartment. Examples are the H3K9 methyltransferase G9a (Chen et al., 2012) and the histone demethylase LSD1/KDM1a (Kerenyi et al., 2013). Interestingly, G9A (Mozzetta et al., 2014) and LSD1 have both been reported to collaborate with EZH2 (Tsai et al., 2010). In human leukemia, stem cell gene expression signatures have been linked to inferior outcomes (Eppert et al., 2011). ETP-ALL has previously been shown to express a stem cell program compared to non-ETP T-ALL (Zhang et al., 2012a). Our findings show that inactivation of the PRC2 component *Ezh2* directly results in the accentuation of an expression program associated with stem cells and early progenitor cells, suggesting a causal link. This is further supported by our findings that overexpression of the stem cell and early progenitor transcriptional regulator *HoxA9* recapitulates many aspects of PRC2 impairment in this model, including the key features of a more immature and accelerated disease in vivo. Despite its clear functional relevance, *HoxA9* is likely not the only component of this stem cell transcriptional program mediating the effect of PRC2 compromise, and other PRC2 target genes are attractive candidates for further study. A better understanding of the regulation of stem cell programs promises the development of more specific targeting of leukemic self-renewal, sparing normal hematopoietic cells.

Another model of human ETP-ALL has recently been published using transfer of *IL7R* mutants and *LMO2* into purified murine DN thymocytes (Treanor et al., 2014). In this model, murine $p19^{-/-}$ DN thymocytes rather than earlier hematopoietic progenitors or HSCs were the targets of transformation, and inactivation of PRC2 components was not employed. Nonetheless, a leukemic phenotype similar to what we describe was observed. These

findings are in keeping with the reported genetic heterogeneity of human ETP-ALL (Zhang et al., 2012a).

Cooperation with and Accentuation of Growth and Survival Signaling by Inactivation of PRC2

In humans, *PRC2* alterations are frequently found in clinical acute leukemia samples with T cell/myeloid features (Grossmann et al., 2012; Zhang et al., 2012a): For example, in the study by Zhang, 5 of the 11 *NRAS*-mutant and 7 out of 7 *NF1* mutated ETP-ALL cases had an alteration in at least 1 PRC2 component. Genetic alterations impeding PRC2-function are also found in the megakaryoblastic leukemia (AMKL) observed in patients with Down Syndrome (Nikolaev et al., 2013; Yoshida et al., 2013), and in juvenile myelo-monocytic AML (JMML), a RAS driven disease with pathognomonic activating mutation in *RAS* (mostly *NRAS* and *KRAS*) or inactivating mutations in *PTPN11* or *NF1* (Stieglitz et al., 2015). Rare *EZH2*-alterations have been described in adult AML (Cancer Genome Atlas Research Network, 2013) (3 out of 200 analyzed samples) and, interestingly, 2 out of these 3 samples had co-occurring mutations in *KRAS* or *NRAS*. Very recently, cooperation between the RAS pathway and PRC2 inactivation has also been demonstrated for some solid tumors (De Raedt et al., 2014). These clinical and experimental data, together with our findings, support the concept that RAS signaling cooperates with PRC2 compromise in cellular transformation and support the relevance of our findings to human malignancy.

JAK/STAT signaling is emerging as an important pathogenic factor in hematopoietic malignancies. Mutations of *JAK* genes or the IL7 receptor have been implicated in T-lineage ALL (Degryse et al., 2014; Zhang et al., 2012a). Hyperactivation of STAT3 in response to growth factors has been linked to inferior survival in human pediatric AML (Redell et al., 2013). Importantly, signaling abnormalities observed in human ETP-ALL, such as *SH2B3* alterations and *FLT3-ITD*, have been linked to hyperactive STAT3 signaling (Mead et al., 2013; Perez-Garcia et al., 2013). Our data indicate that inactivation of *Ezh2* leads to accentuated phosphorylation of STAT3 on tyrosine 705, which was associated with an increase in expression of *Il6ra* and hypersensitive STAT3 phosphorylation in response to IL6.

Although we cannot completely rule out off-target effects, our studies using three different inhibitors of JAK/STAT signaling strongly suggest functional importance of JAK/STAT signaling in our model. These data are significant in several respects: (1) our findings directly link inactivation in an epigenetic modifier to a biochemical signaling change; (2) PRC2 inactivation simultaneously induces two poor prognostic features, a stem cell transcriptional signature and hyperactivation of STAT3 in response to growth factors, both independently linked to poor outcome; and (3) while the JAK/STAT pathway is clearly active and functional in our model, pharmacologic inhibition may be more challenging due to increased levels of STAT phosphorylation to be overcome. In addition, possibly alternate signaling pathways in addition to IL6/IL6RA, such as the accentuated RAS transcriptional signature, will need to be considered.

The relationship of STAT3 signaling and EZH2 is complex. EZH2-mediated methylation of STAT3 has been reported to be required for STAT3Y705 phosphorylation in glioma cells

(Kim et al., 2013). In colon cancer cells, this dependency was not found, but EZH2-mediated methylation of STAT3 was found to be important for full induction of a subset of STAT3 target genes (Dasgupta et al., 2015). Differences in cell type and experimental setup may account for these differences. In our model, inactivation of *Ezh2* resulted in a net positive enrichment of canonical STAT3 target genes (Figures S5D and S5E).

PRC2 As a Therapeutic Target in Cancer Therapy

Context dependence will need to be considered in the use of drugs targeting epigenetic modifiers: pharmacologic inhibition of EZH2 is a highly promising strategy in carefully selected target diseases (Kim et al., 2015; Knutson et al., 2012, 2013; LaFave et al., 2015; McCabe et al., 2012) and may have potential benefit in the treatment of *MLL*-rearranged leukemia (Danis et al., 2015; Neff et al., 2012; Shi et al., 2013; Tanaka et al., 2012; Xu et al., 2015). Our data provide additional evidence that rational selection of target diseases based on molecular features will be an important determinant of success for the next generation of epigenetic cancer therapies.

In summary, our data link inactivation of *Ezh2* to stem cell expression programs and to hyperactive cytokine signaling through STAT3, both features known to be associated with inferior clinical outcome. Our data clarify the role of *Ezh2* in ETP-ALL and support the use of therapies targeting JAK/STAT signaling, as recently suggested by Teachy and colleagues in ETP-ALL patient samples (Maude et al., 2015) and by Sorrentino and colleagues in a murine model of ETP-ALL (Treanor et al., 2014). These prior studies did not investigate *Ezh2* mutant samples. Our data suggest that *EZH2*-mutated cases, which are specifically associated with poor clinical outcomes (Zhang et al., 2012a), may also potentially benefit from modulation of the JAK/STAT signaling pathway, especially if synergistic compounds can be identified. However, inhibiting the accentuated signaling may require somewhat higher doses in PRC2 mutant versus wild-type cells, and close attention will need to be paid in clinical studies to ensure target inhibition in this subgroup. Our work thus provides mechanistic insights into the association of PRC2 with poor prognostic features, and has critical implications for the study of JAK/STAT pathway inhibition in T-ALL.

EXPERIMENTAL PROCEDURES

For published plasmids used, antibodies, primer sequences, gene sets, gene lists (Table S1), and additional experimental details, please refer to Supplemental Experimental Procedures.

Mice

Animals were maintained at the Animal Research Facility at the University of Colorado Anschutz Medical Campus. Animal experiments were approved by the Internal Animal Care and Use Committee at the University of Colorado Denver Anschutz Medical Campus. All mice were maintained on a fully backcrossed C57BL/6 background. See Supplemental Experimental Procedures for mouse genotypes.

Generation of Transformed Murine Cells and Leukemia

MSCV-Ras-pgk-puro was created by subcloning human *NRASQ61K* sequences (Addgene plasmid 12543, Channing Der lab) as a BamH1 fragment into the MSCV-puro vector. See Supplemental Experimental Procedures for published plasmids. $LIN^{-}SCA1^{+}KIT^{+}$ (LSK-) cells were sorted from donor bone marrow using a MoFlo flow sorter (Beckman Coulter) were prestimulated in liquid culture in the presence of murine SCF (20 ng/ml), FLT3L (20 ng/ml), IL6 (20 ng/ml), and TPO (10 ng/ml) (Peprotec) and then transduced on Retronectin-coated (Takara) plates. Cells were sorted for expression of *GFP* or *YFP* and were selected in the presence of Puromycin on OP9-DL1 cells carrying a resistance gene for puromycin in the presence of FLT3L (5 ng/ml), SCF (5 ng/ml), and IL7 (1 ng/ml). Cells expanded for 14–21 days were then injected into syngeneic sublethally (600 cGy) irradiated recipients. Cell growth and viability were followed by serial cell counts. Antibodies used for flow cytometry and immunoblot detection and qPCR primers are detailed in Supplemental Experimental Procedures.

Western Blotting

Proteins for histone blots were harvested using acid extraction (see Supplemental Experimental Procedures). Proteins for non-histone protein blots were harvested using RIPA-buffer including cOmplete mini protease inhibitor cocktail (Roche) and, for phospho-blots, phosSTOP phosphatase inhibitor (Roche), according to the manufacturer's instructions. Protein was separated on a 10% Bis-Tris Gel (Nupage; Invitrogen) and blotted using the “iblot” dry transfer system (Invitrogen).

qRT-PCR

qRT-PCR was used to confirm expression of candidate genes identified by RNA sequencing. RNA was harvested from NRASQ61K-transformed sorted fluorochrome-positive (GFP for $Ezh2^{f/f}$ and $Eed^{f/f}$ and YFP for $Ezh2^{D/D}$ and $Eed^{D/D}$) blasts isolated from leukemic spleens, using RNeasy mini columns (QIAGEN). Individual RNA samples were reverse transcribed and qRT-PCR was run in triplicate using SYBR green. Ratios were calculated using the method described by Pfaffl (Pfaffl, 2001). The Student's t test was performed on log-transformed ratios of gene of interest/internal control (*Hprt*) using GraphPad 6 software.

Chromatin Immunoprecipitation followed by Next-Generation Sequencing

ChIP for H3K27me3 in murine leukemias was performed using rabbit monoclonal antibody clone (C36B11) from Cell Signaling similarly as described elsewhere (Neff et al., 2012). ChIP DNA libraries were made using the Nugen Ovation Ultralow system V2, followed by next-generation sequencing on an Illumina HiSeq2000 at the Genomics Core of the University of Colorado Anschutz Campus. See Supplemental Experimental Procedures for details on data analysis.

Gene Set Enrichment Analysis

GSEA was performed as described previously (Subramanian et al., 2005) using pre-ranked gene lists as input files. Construction of gene sets used is described in Supplemental Experimental Procedures, and the gene sets are listed in Table S1.

Supplementary Material

Refer to Web version on PubMed Central for supplementary material.

ACKNOWLEDGMENTS

We thank Karen Helm and the staff at the flow cytometry core for assistance with FACS and cell sorting. We thank Katrina Diener and Ted Shade at the Genomics core of the University of Colorado AMC. We thank Ken Jones at the Bioinformatics core for help with Illumina data analysis. We thank Tracy Haney and Holly Goold for animal Husbandry. We thank Patricia Ernst and Craig Jordan for critically reading the manuscript. This work was supported by National Cancer Institute (NCI) grant K08CA154777 (T.N.); start-up funds from University of Colorado Denver, Section for Pediatric Hematology/Oncology, and the Children's Hospital Colorado Research Institute (T.N.); the Cancer League Colorado (T.N.); the Sidney Kimmel Foundation for Cancer Research (T.N.); National Heart, Lung, and Blood Institute grant K08HL102264 (K.M.B.); and NCI grant P30CA046934 (Shared Resource of the University of Colorado Cancer Center).

REFERENCES

Béguelin W, Popovic R, Teater M, Jiang Y, Bunting KL, Rosen M, Shen H, Yang SN, Wang L, Ezponda T, et al. EZH2 is required for germinal center formation and somatic EZH2 mutations promote lymphoid transformation. Cancer Cell. 2013; 23:677–692. [PubMed: 23680150]

Bell JJ, Bhandoola A. The earliest thymic progenitors for T cells possess myeloid lineage potential. Nature. 2008; 452:764–767. [PubMed: 18401411]

Bernt KM, Zhu N, Sinha AU, Vempati S, Faber J, Krivtsov AV, Feng Z, Punt N, Daigle A, Bullinger L, et al. MLL-rearranged leukemia is dependent on aberrant H3K79 methylation by DOT1L. Cancer Cell. 2011; 20:66–78. [PubMed: 21741597]

Caganova M, Carrisi C, Varano G, Mainoldi F, Zanardi F, Germain PL, George L, Alberghini F, Ferrarini L, Talukder AK, et al. Germinal center dysregulation by histone methyltransferase EZH2 promotes lymphomagenesis. J. Clin. Invest. 2013; 123:5009–5022. [PubMed: 24200695]

Cancer Genome Atlas Research Network. Genomic and epigenomic landscapes of adult de novo acute myeloid leukemia. N. Engl. J. Med. 2013; 368:2059–2074. [PubMed: 23634996]

Chambers SM, Boles NC, Lin KY, Tierney MP, Bowman TV, Bradfute SB, Chen AJ, Merchant AA, Sirin O, Weksberg DC, et al. Hematopoietic fingerprints: an expression database of stem cells and their progeny. Cell Stem Cell. 2007; 1:578–591. [PubMed: 18371395]

Chen X, Skutt-Kakaria K, Davison J, Ou YL, Choi E, Malik P, Loeb K, Wood B, Georges G, Torok-Storb B, Paddison PJ. G9a/GLP-dependent histone H3K9me2 patterning during human hematopoietic stem cell lineage commitment. Genes Dev. 2012; 26:2499–2511. [PubMed: 23105005]

Coustan-Smith E, Mullighan CG, Onciu M, Behm FG, Raimondi SC, Pei D, Cheng C, Su X, Rubnitz JE, Basso G, et al. Early T-cell precursor leukaemia: a subtype of very high-risk acute lymphoblastic leukaemia. Lancet Oncol. 2009; 10:147–156. [PubMed: 19147408]

Danis E, Yamauchi T, Echanique K, Haladyna J, Kalkur R, Riedel S, Zhu N, Xie H, Bernt KM, Orkin SH, et al. Inactivation of Eed impedes MLL-AF9-mediated leukemogenesis through Cdkn2a-dependent and Cdkn2a-independent mechanisms in a murine model. Exp. Hematol. 2015; 43:930–935. [PubMed: 26118502]

Dasgupta M, Dermawan JK, Willard B, Stark GR. STAT3-driven transcription depends upon the dimethylation of K49 by EZH2. Proc. Natl. Acad. Sci. USA. 2015; 112:3985–3990. [PubMed: 25767098]

De Raedt T, Beert E, Pasmant E, Luscan A, Brems H, Ortonne N, Helin K, Hornick JL, Mautner V, Kehrer-Sawatzki H, et al. PRC2 loss amplifies Ras-driven transcription and confers sensitivity to BRD4-based therapies. Nature. 2014; 514:247–251. [PubMed: 25119042]

Degryse S, de Bock CE, Cox L, Demeyer S, Gielen O, Mentens N, Jacobs K, Geerdens E, Gianfelici V, Hulselmans G, et al. JAK3 mutants transform hematopoietic cells through JAK1 activation, causing T-cell acute lymphoblastic leukemia in a mouse model. Blood. 2014; 124:3092–3100. [PubMed: 25193870]

Eppert K, Takenaka K, Lechman ER, Waldron L, Nilsson B, van Galen P, Metzeler KH, Poeppl A, Ling V, Beyene J, et al. Stem cell gene expression programs influence clinical outcome in human leukemia. Nat. Med. 2011; 17:1086–1093. [PubMed: 21873988]

Ernst T, Chase AJ, Score J, Hidalgo-Curtis CE, Bryant C, Jones AV, Waghorn K, Zoi K, Ross FM, Reiter A, et al. Inactivating mutations of the histone methyltransferase gene EZH2 in myeloid disorders. Nat. Genet. 2010; 42:722–726. [PubMed: 20601953]

Feng J, Liu T, Qin B, Zhang Y, Liu XS. Identifying ChIP-seq enrichment using MACS. Nat. Protoc. 2012; 7:1728–1740. [PubMed: 22936215]

Grossmann V, Bacher U, Kohlmann A, Artusi V, Klein HU, Dugas M, Schnittger S, Alpermann T, Kern W, Haferlach T, Haferlach C. EZH2 mutations and their association with PICALM-MLLT10 positive acute leukaemia. Br. J. Haematol. 2012; 157:387–390. [PubMed: 22235851]

Guglielmelli P, Biamonte F, Score J, Hidalgo-Curtis C, Cervantes F, Maffioli M, Fanelli T, Ernst T, Winkelman N, Jones AV, et al. EZH2 mutational status predicts poor survival in myelofibrosis. Blood. 2011; 118:5227–5234. [PubMed: 21921040]

Haydu JE, Ferrando AA. Early T-cell precursor acute lymphoblastic leukaemia. Curr. Opin. Hematol. 2013; 20:369–373. [PubMed: 23695450]

Hidalgo I, Herrera-Merchan A, Ligos JM, Carramolino L, Nuñez J, Martinez F, Dominguez O, Torres M, Gonzalez S. Ezh1 is required for hematopoietic stem cell maintenance and prevents senescence-like cell cycle arrest. Cell Stem Cell. 2012; 11:649–662. [PubMed: 23122289]

Kerenyi MA, Shao Z, Hsu YJ, Guo G, Luc S, O'Brien K, Fujiwara Y, Peng C, Nguyen M, Orkin SH. Histone demethylase Lsd1 represses hematopoietic stem and progenitor cell signatures during blood cell maturation. eLife. 2013; 2:e00633. [PubMed: 23795291]

Kim E, Kim M, Woo DH, Shin Y, Shin J, Chang N, Oh YT, Kim H, Rheey J, Nakano I, et al. Phosphorylation of EZH2 activates STAT3 signaling via STAT3 methylation and promotes tumorigenicity of glioblastoma stem-like cells. Cancer Cell. 2013; 23:839–852. [PubMed: 23684459]

Kim KH, Kim W, Howard TP, Vazquez F, Tsherniak A, Wu JN, Wang W, Haswell JR, Walensky LD, Hahn WC, et al. SWI/SNF-mutant cancers depend on catalytic and non-catalytic activity of EZH2. Nat. Med. 2015; 21:1491–1496. [PubMed: 26552009]

Knutson SK, Wigle TJ, Warholic NM, Sneeringer CJ, Allain CJ, Klaus CR, Sacks JD, Raimondi A, Majer CR, Song J, et al. A selective inhibitor of EZH2 blocks H3K27 methylation and kills mutant lymphoma cells. Nat. Chem. Biol. 2012; 8:890–896. [PubMed: 23023262]

Knutson SK, Warholic NM, Wigle TJ, Klaus CR, Allain CJ, Raimondi A, Porter Scott M, Chesworth R, Moyer MP, Copeland RA, et al. Durable tumor regression in genetically altered malignant rhabdoid tumors by inhibition of methyltransferase EZH2. Proc. Natl. Acad. Sci. USA. 2013; 110:7922–7927. [PubMed: 23620515]

Krivtsov AV, Twomey D, Feng Z, Stubbs MC, Wang Y, Faber J, Levine JE, Wang J, Hahn WC, Gilliland DG, et al. Transformation from committed progenitor to leukaemia stem cell initiated by MLL-AF9. Nature. 2006; 442:818–822. [PubMed: 16862118]

Krivtsov AV, Figueroa ME, Sinha AU, Stubbs MC, Feng Z, Valk PJ, Delwel R, Dohner K, Bullinger L, Kung AL, et al. Cell of origin determines clinically relevant subtypes of MLL-rearranged AML. Leukemia. 2013; 27:852–860. [PubMed: 23235717]

LaFave LM, Béguelin W, Koche R, Teater M, Spitzer B, Chramiec A, Papalexi E, Keller MD, Hricik T, Konstantinoff K, et al. Loss of BAP1 function leads to EZH2-dependent transformation. Nat. Med. 2015; 21:1344–1349. [PubMed: 26437366]

Laugesen A, Helin K. Chromatin repressive complexes in stem cells, development, and cancer. Cell Stem Cell. 2014; 14:735–751. [PubMed: 24905164]

Liu Y, Li PK, Li C, Lin J. Inhibition of STAT3 signaling blocks the anti-apoptotic activity of IL-6 in human liver cancer cells. J. Biol. Chem. 2010; 285:27429–27439. [PubMed: 20562100]

Margueron R, Li G, Sarma K, Blais A, Zavadil J, Woodcock CL, Dynlacht BD, Reinberg D. Ezh1 and Ezh2 maintain repressive chromatin through different mechanisms. Mol. Cell. 2008; 32:503–518. [PubMed: 19026781]

Maude SL, Dolai S, Delgado-Martin C, Vincent T, Robbins A, Selvanathan A, Ryan T, Hall J, Wood AC, Tasian SK, et al. Efficacy of JAK/STAT pathway inhibition in murine xenograft models of early T-cell precursor (ETP) acute lymphoblastic leukemia. Blood. 2015; 125:1759–1767. [PubMed: 25645356]

McCabe MT, Ott HM, Ganji G, Korenchuk S, Thompson C, Van Aller GS, Liu Y, Graves AP, Della Pietra A 3rd, Diaz E, et al. EZH2 inhibition as a therapeutic strategy for lymphoma with EZH2-activating mutations. Nature. 2012; 492:108–112. [PubMed: 23051747]

McLemore ML, Grewal S, Liu F, Archambault A, Poursine-Laurent J, Haug J, Link DC. STAT-3 activation is required for normal G-CSF-dependent proliferation and granulocytic differentiation. Immunity. 2001; 14:193–204. [PubMed: 11239451]

Mead AJ, Kharazi S, Atkinson D, Macaulay I, Pecquet C, Loughran S, Lutteropp M, Woll P, Chowdhury O, Luc S, et al. FLT3-ITDs instruct a myeloid differentiation and transformation bias in lymphomyeloid multipotent progenitors. Cell Rep. 2013; 3:1766–1776. [PubMed: 23727242]

Mozzetta C, Pontis J, Fritsch L, Robin P, Portoso M, Proux C, Margueron R, Ait-Si-Ali S. The histone H3 lysine 9 methyltransferases G9a and GLP regulate polycomb repressive complex 2-mediated gene silencing. Mol. Cell. 2014; 53:277–289. [PubMed: 24389103]

Muto T, Sashida G, Oshima M, Wendt GR, Mochizuki-Kashio M, Nagata Y, Sanada M, Miyagi S, Saraya A, Kamio A, et al. Concurrent loss of Ezh2 and Tet2 cooperates in the pathogenesis of myelodysplastic disorders. J. Exp. Med. 2013; 210:2627–2639. [PubMed: 24218139]

Neff T, Sinha AU, Kluk MJ, Zhu N, Khattab MH, Stein L, Xie H, Orkin SH, Armstrong SA. Polycomb repressive complex 2 is required for MLL-AF9 leukemia. Proc. Natl. Acad. Sci. USA. 2012; 109:5028–5033. [PubMed: 22396593]

Nikolaev SI, Santoni F, Vannier A, Falconnet E, Giarin E, Basso G, Hoischen A, Veltman JA, Groet J, Nizetic D, Antonarakis SE. Exome sequencing identifies putative drivers of progression of transient myeloproliferative disorder to AMKL in infants with Down syndrome. Blood. 2013; 122:554–561. [PubMed: 23733339]

Nikoloski G, Langemeijer SM, Kuiper RP, Knops R, Massop M, Tönnissen ER, van der Heijden A, Scheele TN, Vandenberghe P, de Witte T, et al. Somatic mutations of the histone methyltransferase gene EZH2 in myelodysplastic syndromes. Nat. Genet. 2010; 42:665–667. [PubMed: 20601954]

Novershtern N, Subramanian A, Lawton LN, Mak RH, Haining WN, McConkey ME, Habib N, Yosef N, Chang CY, Shay T, et al. Densely interconnected transcriptional circuits control cell states in human hematopoiesis. Cell. 2011; 144:296–309. [PubMed: 21241896]

Ntziachristos P, Tsirigos A, Van Vlierberghe P, Nedjic J, Trimarchi T, Flaherty MS, Ferres-Marco D, da Ros V, Tang Z, Siegle J, et al. Genetic inactivation of the polycomb repressive complex 2 in T cell acute lymphoblastic leukemia. Nat. Med. 2012; 18:298–301. [PubMed: 22237151]

Oguro H, Yuan J, Tanaka S, Miyagi S, Mochizuki-Kashio M, Ichikawa H, Yamazaki S, Koseki H, Nakauchi H, Iwama A. Lethal myelofibrosis induced by Bmi1-deficient hematopoietic cells unveils a tumor suppressor function of the polycomb group genes. J. Exp. Med. 2012; 209:445–454. [PubMed: 22351929]

Okosun J, Bödör C, Wang J, Araf S, Yang CY, Pan C, Boller S, Cittaro D, Bozek M, Iqbal S, et al. Integrated genomic analysis identifies recurrent mutations and evolution patterns driving the initiation and progression of follicular lymphoma. Nat. Genet. 2014; 46:176–181. [PubMed: 24362818]

Oravecz A, Apostolov A, Polak K, Jost B, Le Gras S, Chan S, Kastner P. Ikaros mediates gene silencing in T cells through Polycomb repressive complex 2. Nat. Commun. 2015; 6:8823. [PubMed: 26549758]

Pasini D, Bracken AP, Hansen JB, Capillo M, Helin K. The polycomb group protein Suz12 is required for embryonic stem cell differentiation. Mol. Cell. Biol. 2007; 27:3769–3779. [PubMed: 17339329]

Perez-Garcia A, Ambesi-Impiombato A, Hadler M, Rigo I, LeDuc CA, Kelly K, Jalas C, Paietta E, Racevskis J, Rowe JM, et al. Genetic loss of SH2B3 in acute lymphoblastic leukemia. Blood. 2013; 122:2425–2432. [PubMed: 23908464]

Pfaffl MW. A new mathematical model for relative quantification in real-time RT-PCR. Nucleic Acids Res. 2001; 29:e45. [PubMed: 11328886]

Redell MS, Ruiz MJ, Gerbing RB, Alonzo TA, Lange BJ, Tweardy DJ, Meshinchi S, Children's Oncology Group. FACS analysis of Stat3/5 signaling reveals sensitivity to G-CSF and IL-6 as a significant prognostic factor in pediatric AML: a Children's Oncology Group report. Blood. 2013; 121:1083–1093. [PubMed: 23243289]

Schmitt TM, Zúñiga-Pflücker JC. Induction of T cell development from hematopoietic progenitor cells by delta-like-1 in vitro. Immunity. 2002; 17:749–756. [PubMed: 12479821]

Serrano M, Lee H, Chin L, Cordon-Cardo C, Beach D, DePinho RA. Role of the INK4a locus in tumor suppression and cell mortality. Cell. 1996; 85:27–37. [PubMed: 8620534]

Shen X, Liu Y, Hsu YJ, Fujiwara Y, Kim J, Mao X, Yuan GC, Orkin SH. EZH1 mediates methylation on histone H3 lysine 27 and complements EZH2 in maintaining stem cell identity and executing pluripotency. Mol. Cell. 2008; 32:491–502. [PubMed: 19026780]

Shi J, Wang E, Zuber J, Rappaport A, Taylor M, Johns C, Lowe SW, Vakoc CR. The Polycomb complex PRC2 supports aberrant self-renewal in a mouse model of MLL-AF9;Nras(G12D) acute myeloid leukemia. Oncogene. 2013; 32:930–938. [PubMed: 22469984]

Shimozaki K, Nakajima K, Hirano T, Nagata S. Involvement of STAT3 in the granulocyte colony-stimulating factor-induced differentiation of myeloid cells. J. Biol. Chem. 1997; 272:25184–25189. [PubMed: 9312131]

Simon C, Chagraoui J, Krosl J, Gendron P, Wilhelm B, Lemieux S, Boucher G, Chagnon P, Drouin S, Lambert R, et al. A key role for EZH2 and associated genes in mouse and human adult T-cell acute leukemia. Genes Dev. 2012; 26:651–656. [PubMed: 22431509]

Sneeringer CJ, Scott MP, Kuntz KW, Knutson SK, Pollock RM, Richon VM, Copeland RA. Coordinated activities of wild-type plus mutant EZH2 drive tumor-associated hypertrimethylation of lysine 27 on histone H3 (H3K27) in human B-cell lymphomas. Proc. Natl. Acad. Sci. USA. 2010; 107:20980–20985. [PubMed: 21078963]

Srinivas S, Watanabe T, Lin CS, William CM, Tanabe Y, Jessell TM, Costantini F. Cre reporter strains produced by targeted insertion of EYFP and ECFP into the ROSA26 locus. BMC Dev. Biol. 2001; 1:4. [PubMed: 11299042]

Stieglitz E, Taylor-Weiner AN, Chang TY, Gelston LC, Wang YD, Mazor T, Esquivel E, Yu A, Seepo S, Olsen SR, et al. The genomic landscape of juvenile myelomonocytic leukemia. Nat. Genet. 2015; 47:1326–1333. [PubMed: 26457647]

Su IH, Dobenecker MW, Dickinson E, Oser M, Basavaraj A, Marqueron R, Viale A, Reinberg D, Wülfing C, Tarakhovsky A. Polycomb group protein ezh2 controls actin polymerization and cell signaling. Cell. 2005; 121:425–436. [PubMed: 15882624]

Subramanian A, Tamayo P, Mootha VK, Mukherjee S, Ebert BL, Gillette MA, Paulovich A, Pomeroy SL, Golub TR, Lander ES, Mesirov JP. Gene set enrichment analysis: a knowledge-based approach for interpreting genome-wide expression profiles. Proc. Natl. Acad. Sci. USA. 2005; 102:15545–15550. [PubMed: 16199517]

Tanaka S, Miyagi S, Sashida G, Chiba T, Yuan J, Mochizuki-Kashio M, Suzuki Y, Sugano S, Nakaseko C, Yokote K, et al. Ezh2 augments leukemogenicity by reinforcing differentiation blockage in acute myeloid leukemia. Blood. 2012; 120:1107–1117. [PubMed: 22677129]

Treanor LM, Zhou S, Janke L, Churchman ML, Ma Z, Lu T, Chen SC, Mullighan CG, Sorrentino BP. Interleukin-7 receptor mutants initiate early T cell precursor leukemia in murine thymocyte progenitors with multipotent potential. J. Exp. Med. 2014; 211:701–713. [PubMed: 24687960]

Tsai MC, Manor O, Wan Y, Mosammaparast N, Wang JK, Lan F, Shi Y, Segal E, Chang HY. Long noncoding RNA as modular scaffold of histone modification complexes. Science. 2010; 329:689–693. [PubMed: 20616235]

Varambally S, Dhanasekaran SM, Zhou M, Barrette TR, Kumar-Sinha C, Sanda MG, Ghosh D, Pienta KJ, Sewalt RG, Otte AP, et al. The polycomb group protein EZH2 is involved in progression of prostate cancer. Nature. 2002; 419:624–629. [PubMed: 12374981]

Velu CS, Chaubey A, Phelan JD, Horman SR, Wunderlich M, Guzman ML, Jegga AG, Zeleznik-Le NJ, Chen J, Mulloy JC, et al. Therapeutic antagonists of microRNAs deplete leukemia-initiating cell activity. J. Clin. Invest. 2014; 124:222–236. [PubMed: 24334453]

Verhaak RG, Wouters BJ, Erpelinck CA, Abbas S, Beverloo HB, Lugthart S, Löwenberg B, Delwel R, Valk PJ. Prediction of molecular subtypes in acute myeloid leukemia based on gene expression profiling. Haematologica. 2009; 94:131–134. [PubMed: 18838472]

Wada H, Masuda K, Satoh R, Kakugawa K, Ikawa T, Katsura Y, Kawamoto H. Adult T-cell progenitors retain myeloid potential. Nature. 2008; 452:768–772. [PubMed: 18401412]

Xie H, Xu J, Hsu JH, Nguyen M, Fujiwara Y, Peng C, Orkin SH. Polycomb repressive complex 2 regulates normal hematopoietic stem cell function in a developmental-stage-specific manner. Cell Stem Cell. 2014; 14:68–80. [PubMed: 24239285]

Xu B, On DM, Ma A, Parton T, Konze KD, Pattenden SG, Allison DF, Cai L, Rockowitz S, Liu S, et al. Selective inhibition of EZH2 and EZH1 enzymatic activity by a small molecule suppresses MLL-rearranged leukemia. Blood. 2015; 125:346–357. [PubMed: 25395428]

Yoshida K, Toki T, Okuno Y, Kanezaki R, Shiraishi Y, Sato-Otsubo A, Sanada M, Park MJ, Terui K, Suzuki H, et al. The landscape of somatic mutations in Down syndrome-related myeloid disorders. Nat. Genet. 2013; 45:1293–1299. [PubMed: 24056718]

Zhang J, Ding L, Holmfeldt L, Wu G, Heatley SL, Payne-Turner D, Easton J, Chen X, Wang J, Rusch M, et al. The genetic basis of early T-cell precursor acute lymphoblastic leukaemia. Nature. 2012a; 481:157–163. [PubMed: 22237106]

Zhang JA, Mortazavi A, Williams BA, Wold BJ, Rothenberg EV. Dynamic transformations of genome-wide epigenetic marking and transcriptional control establish T cell identity. Cell. 2012b; 149:467–482. [PubMed: 22500808]

Zhang X, Yue P, Page BD, Li T, Zhao W, Namanja AT, Paladino D, Zhao J, Chen Y, Gunning PT, Turkson J. Orally bioavailable small-molecule inhibitor of transcription factor Stat3 regresses human breast and lung cancer xenografts. Proc. Natl. Acad. Sci. USA. 2012c; 109:9623–9628. [PubMed: 22623533]

Highlights

d Genetic inactivation of *Ezh*2 or *Eed* cooperates with *NRASQ61K* in leukemogenesis

d Inactivation of *Ezh2* enhances a stem-cell-related transcriptional program

d Inactivation of *Ezh2* results in increased STAT3 activation via Y705 phosphorylation

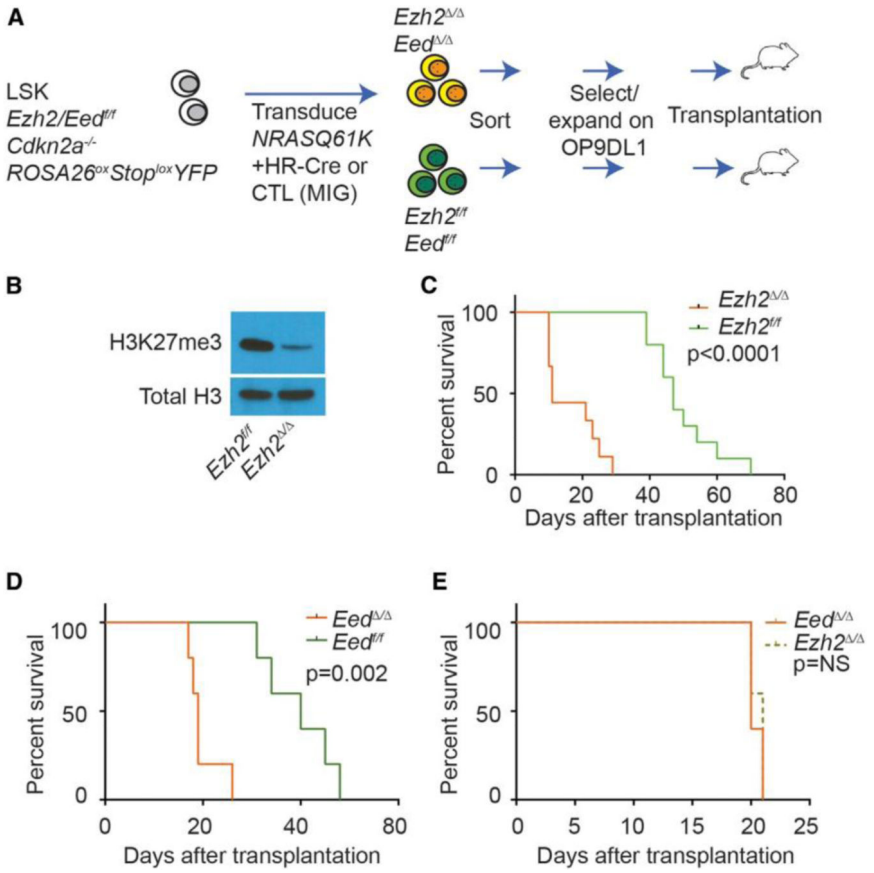

Figure 1. Genetic Inactivation of *Ezh2 or Eed* Cooperates with *NRASQ61K* in the Establishment of Murine Leukemia

(A) Experimental schema.

(B) Inactivation of *Ezh2* results in global decrease in cellular H3K27me3 (western blot).

(C) Significantly shortened survival in recipients of *Ezh2*$^{D/D}$ *Cdkn2a*$^{-/-}$ *NRASQ61K* cells compared to floxed counterparts (n = 10 mice per group; Kaplan-Meier analysis).

(D) Significantly shortened survival in recipients of *Eed*$^{D/D}$ *Cdkn2a*$^{-/-}$ *NRASQ61K* cells compared to floxed counterparts (n = 10 mice per group; Kaplan-Meier analysis).

(E) Direct comparison shows similar survival in recipients of *Ezh2*$^{D/D}$ *Cdkn2a*$^{-/-}$ *NRASQ61K* cells and recipients of *Eed*$^{D/D}$ *Cdkn2a*$^{-/-}$ *NRASQ61K* cells (n = 10 mice per group; Kaplan-Meier analysis). NS, not significant.

See also Figures S1 and S2.

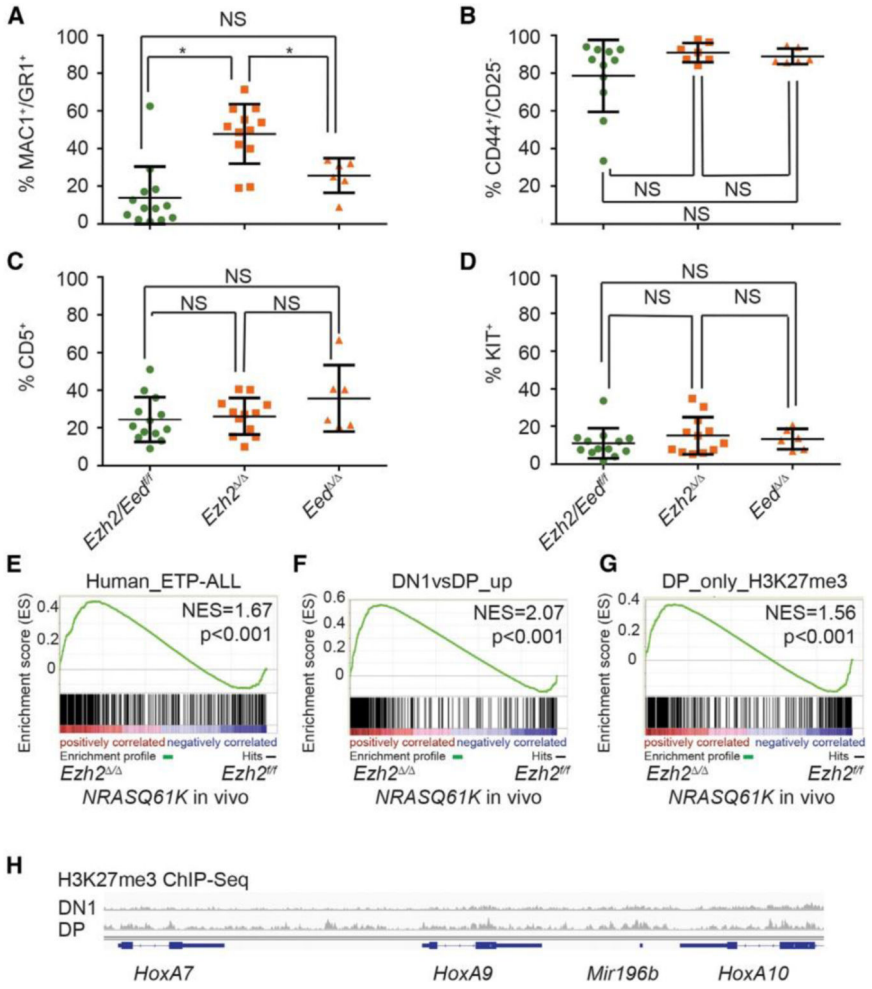

Figure 2. *NRASQ61K* Leukemia Has Phenotypic Features of ETP-ALL and *Ezh2* Controls a Gene Expression Program Characteristic of ETP-ALL and of Physiologic Murine Early Thymic Precursors

(A) Higher proportion of cells double positive (DP) for myeloid markers MAC1 and GR1 in *Ezh2*$^{D/D}$ *Cdkn2a*$^{-/-}$ *NRASQ61K* cells compared to floxed counterparts. Non-significant trend toward higher MAC1/GR1 DP cells in *Eed*$^{D/D}$ *Cdkn2a*$^{-/-}$ *NRASQ61K* cells compared to floxed counterparts.

(B) A majority of splenic *NRASQ61K* leukemic blasts are CD44^{+}/CD25^{-} in all groups.

(C and D) Comparable subset positive expression of CD5 (C) and KIT (D) in all three groups.

(E) Genes highly expressed in human ETP-ALL compared to typical T-ALL are transcriptionally enriched in vivo in *Ezh2*$^{D/D}$ *Cdkn2a*$^{-/-}$ *NRASQ61K* cells compared to floxed counterparts.

(F) Genes highly expressed in mouse DN1 cells compared to DP cells (“DN1vsDP_up” gene set) are transcriptionally enriched in vivo in *Ezh2*$^{D/D}$ *Cdkn2a*$^{-/-}$ *NRASQ61K* cells.

(G) Genes that acquire H3K27me3 in the transition from the DN1 to the DP stage (“DP_only_ H3K27me3” gene set) are transcriptionally enriched in vivo in *Ezh2*$^{D/D}$ *Cdkn2a*$^{-/-}$ *NRASQ61K*.

(H) ChIP-seq peaks in physiological DN1 and DP cells visualized for the genomic locus for the stem cell-associated late *HoxA* cluster as an examples of genes that acquire H3K27me3 in the developmental transition from DN1 to DP (data from Zhang et al., 2012b).
Error bars represent SD. *$p < 0.05$. NS, not significant. See also Figure S3.

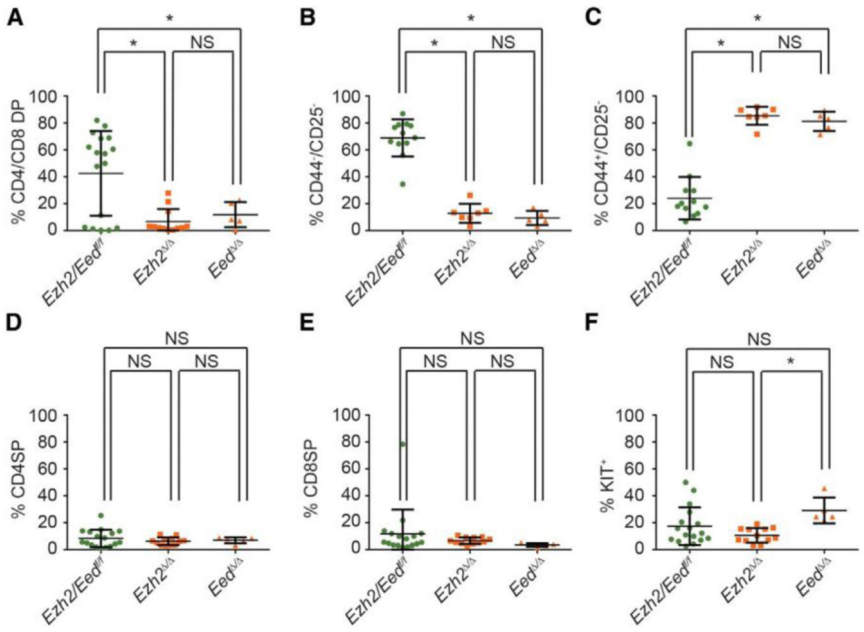

Figure 3. Differentiation Block Is Partially Reversed in the Thymus in *NRASQ61K* Cells with a Fully Functional PRC2 Complex, but Not in *Ezh2*$^{D/D}$ and *Eed*$^{D/D}$ *NRASQ61K* Cells

(A) Significantly higher proportion of CD4/8 DP fluorochrome-positive blasts in the thymus of recipients of *Cdkn2a*$^{-/-}$ *NRASQ61K* cells with a fully functional PRC2.

(B) Significantly lower proportion of CD44^{-}/CD25^{-} blasts in the thymus of recipients of *Ezh2*$^{D/D}$ and *Eed*$^{D/D}$ *Cdkn2a*$^{-/-}$ *NRASQ61K* cells.

(C) Significantly higher proportion of CD44^{+}/CD25^{-} blasts in the thymus of recipients of *Ezh2*$^{D/D}$ and *Eed*$^{D/D}$ *Cdkn2a*$^{-/-}$ *NRASQ61K* cells.

(D) Similar proportion of CD4 single-positive (SP) blasts in the thymus of recipients of *NRASQ61K* cells with a fully functional PRC2 and recipients of *Ezh2*$^{D/D}$ and *Eed*$^{D/D}$ *Cdkn2a*$^{-/-}$ *NRASQ61K* cells.

(E) Similar proportion of CD8 single-positive blasts in the thymus of recipients of *NRASQ61K* cells with a fully functional PRC2 and recipients of *Ezh2*$^{D/D}$ and *Eed*$^{D/D}$ *Cdkn2a*$^{-/-}$ *NRASQ61K* cells.

(F) Similar proportion of KIT positive blasts in the thymus of recipients of *NRASQ61K* cells with a fully functional PRC2 and recipients of *Ezh2*$^{D/D}$ and *Eed*$^{D/D}$ *Cdkn2a*$^{-/-}$ *NRASQ61K* cells (with the *Eed*$^{D/D}$ group showing a small but significant increase compared to *Ezh2*$^{D/D}$ group).

Error bars represent SD. *$p < 0.05$. NS, not significant.

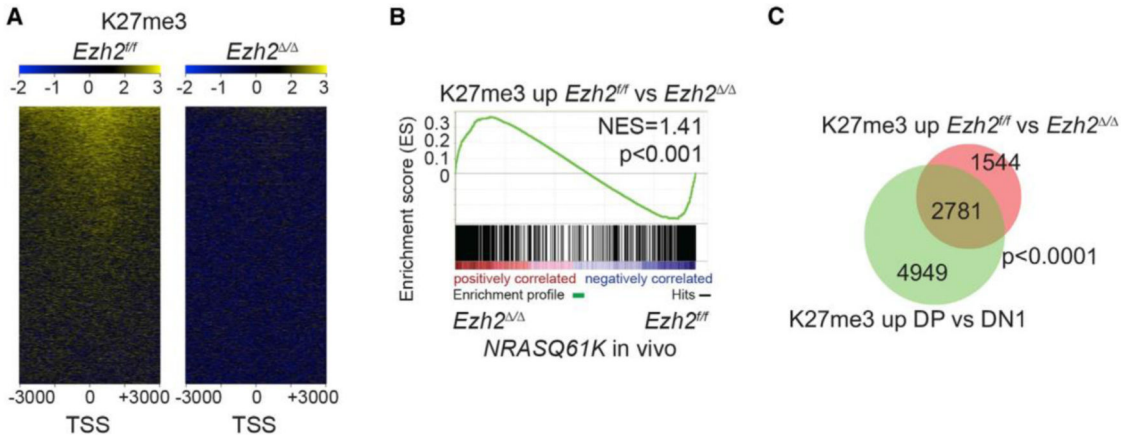

Figure 4. H3K27me3 Changes Correlate with Transcriptional Differences between *Ezh2*$^{f/f}$ and *Ezh2*$^{D/D}$ *Cdkn2a*$^{-/-}$ *NRASQ61K* Cells

(A) H3K27me3 differences between *Ezh2*$^{f/f}$ and *Ezh2*$^{D/D}$ *Cdkn2a*$^{-/-}$ *NRASQ61K* cells (top 5,000 genes). The ranked list of the top 5,000 genes is provided in Table S1.

(B) Enrichment of genes with decrease in H3K27me3 in *Ezh2*$^{D/D}$ *Cdkn2a*$^{-/-}$ *NRASQ61K* cells.

(C) Significant overlap between genes with loss of H3K27me3 after inactivation of *Ezh2* and genes acquiring H3K27me3 in the transition from mouse DN1 to mouse DP cells.

See also Figure S7.

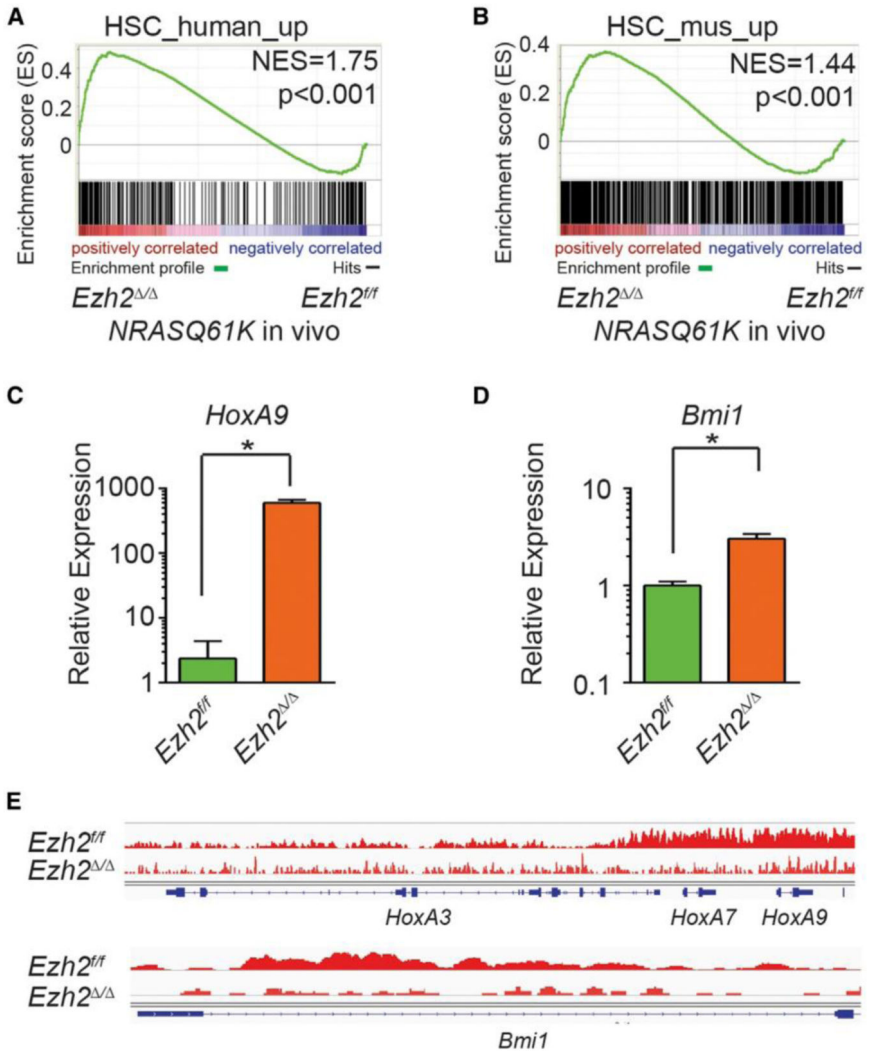

Figure 5. PRC2 Controls a Stem Cell/Early Progenitor Cell Gene Expression Program in Hematopoietic Differentiation

(A) Genes highly expressed in human hematopoietic stem cells are enriched in vivo in *Ezh2*$^{D/D}$ *Cdkn2a*$^{-/-}$ *NRASQ61K* cells compared to their floxed counterparts.

(B) Genes highly expressed in mouse hematopoietic stem cells are enriched in vivo in *Ezh2*$^{D/D}$ *Cdkn2a*$^{-/-}$ *NRASQ61K* cells compared to their floxed counterparts.

(C) *HoxA9* is significantly higher expressed in vivo in *Ezh2*$^{D/D}$ *Cdkn2a*$^{-/-}$ *NRASQ61K* cells compared to their floxed counterparts (Ezh2$^{f/f}$ n = 3, Ezh2$^{D/D}$ n = 4, qRT-PCR).

(D) *Bmi1* is significantly higher expressed in vivo in *Ezh2*$^{D/D}$ *Cdkn2a*$^{-/-}$ *NRASQ61K* cells compared to their floxed counterparts (Ezh2$^{f/f}$ n = 3, Ezh2$^{D/D}$ n = 4, qRT-PCR).

(E) ChIP-seq peaks visualized for the genomic locus for the stem-cell-associated late *HoxA*-cluster and the stem-cell-associated gene *Bmi1* as examples of genes that lose H3K27me3 after inactivation of Ezh2.

Error bars represent SD. *p < 0.05.

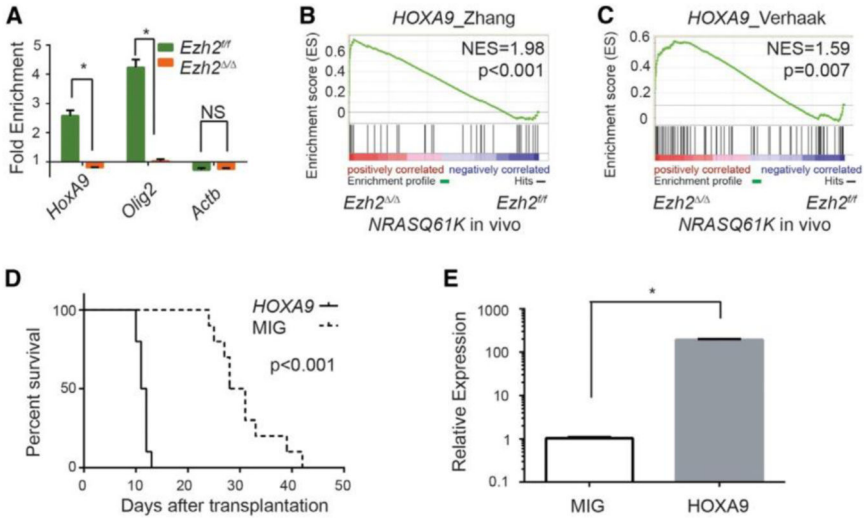

Figure 6. Accentuation of a Developmentally Regulated *HOXA9*-Correlated Gene Expression in *Ezh2*$^{D/D}$ *Cdkn2a*$^{-/-}$ *NRASQ61K* Cells

(A) Increased H3K27me3 enrichment as measured by ChIP-qPCR at loci for *HoxA9* and the documented PRC2 target *Olig2*, but not b-actin, in *Ezh2*$^{f/f}$ *Cdkn2a*$^{-/-}$ *NRASQ61K* cells compared to *Ezh2*$^{D/D}$ *Cdkn2a*$^{-/-}$ *NRASQ61K* cells.

(B) Genes correlated with *HOXA9* expression in T-ALL are transcriptionally enriched in vivo in *Ezh2*$^{D/D}$ *Cdkn2a*$^{-/-}$ *NRASQ61K* cells compared to their floxed counterparts.

(C) Genes correlated with *HOXA9* expression in AML are transcriptionally enriched in *Ezh2*$^{D/D}$ *Cdkn2a*$^{-/-}$ *NRASQ61K* cells compared to their floxed counterparts.

(D) Forced expression of *HoxA9* synergizes with *NRASQ61K* in leukemogenesis in the presence of an intact *Ezh2* locus.

(E) Increased expression of *HoxA9* in MSCV-HoxA9-i-GFP (HOXA9) compared to MSCV-i-GFP (MIG) transduced cells (qRT-PCR).

Error bars represent SD. *p < 0.05. See also Figure S4.

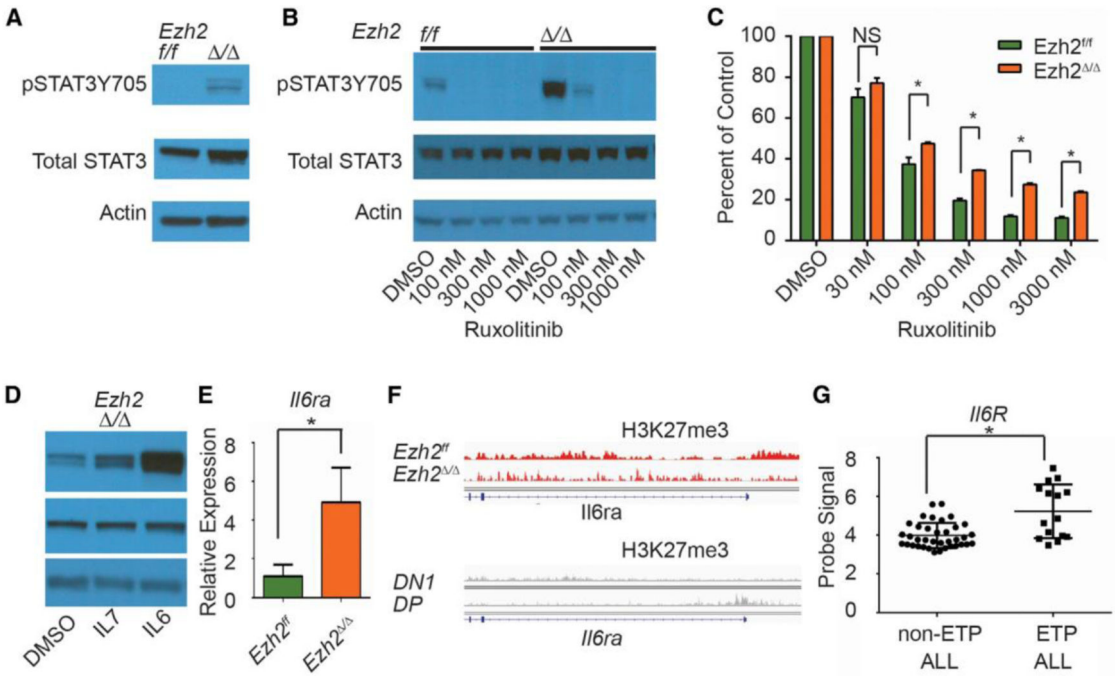

Figure 7. *Ezh2*-Inactivation Leads to Accentuated Growth/Survival Signaling in *NRASQ61K* Leukemia

(A) Phospho-western blotting reveals increased STAT3Y705 phosphorylation in *Ezh2*$^{D/D}$ *Cdkn2a*$^{-/-}$ *NRASQ61K* cells compared to their floxed counterparts.

(B) STAT3Y705 phosphorylation is inhibited by ruxolitinib in a dose-dependent manner in *Ezh2*$^{f/f}$ *Cdkn2a*$^{-/-}$ *NRASQ61K* and *Ezh2*$^{D/D}$ *Cdkn2a*$^{-/-}$ *NRASQ61K* cells.

(C) Growth of *Ezh2*$^{f/f}$ *Cdkn2a*$^{-/-}$ *NRASQ61K* and *Ezh2*$^{D/D}$ *Cdkn2a*$^{-/-}$ *NRASQ61K* cells is inhibited by ruxolitinib in a dose-dependent manner.

(D) Exaggerated response to IL6 stimulation in *Ezh2*$^{D/D}$ *Cdkn2a*$^{-/-}$ *NRASQ61K* cells growth factor starved for 8 hr.

(E) Increased level of *Il6ra* expression in *Ezh2*$^{D/D}$ *Cdkn2a*$^{-/-}$ *NRASQ61K* cells.

(F) Increased H3K27me3 at the *Il6ra* locus in *Ezh2*$^{f/f}$ *Cdkn2a*$^{-/-}$ *NRASQ61K* cells compared to *Ezh2*$^{D/D}$ *Cdkn2a*$^{-/-}$ *NRASQ61K* cells and in normal mouse DP cells compared to DN1 cells.

(G) Significantly increased *IL6RA* expression in human ETP-ALL compared to non-ETP ALL.

Error bars represent SD. *p < 0.05. NS, not significant. See also Figures S5 and S6.